Fungal disease dynamics in insect societies: optimal killing rates and the ambivalent effect of high social interaction rates

Sebastian Novak* and Sylvia Cremer*

*IST Austria (Institute of Science and Technology Austria), Am Campus 1, 3400 Klosterneuburg, Austria

Accepted Manuscript, *Journal of Theoretical Biology*, doi:10.1016/j.jtbi.2015.02.018

Abstract

Entomopathogenic fungi are potent biocontrol agents that are widely used against insect pests, many of which are social insects. Nevertheless, theoretical investigations of their particular life history are scarce. We develop a model that takes into account the main distinguishing features between traditionally studied diseases and obligate killing pathogens, like the (biocontrol-relevant) insect-pathogenic fungi *Metarhizium* and *Beauveria*. First, obligate killing entomopathogenic fungi produce new infectious particles (conidiospores) only after host death and not yet on the living host. Second, the killing rates of entomopathogenic fungi depend strongly on the initial exposure dosage, thus we explicitly consider the pathogen load of individual hosts. Further, we make the model applicable not only to solitary host species, but also to group living species by incorporating social interactions between hosts, like the collective disease defences of insect societies. Our results identify the optimal killing rate for the pathogen that minimizes its invasion threshold. Furthermore, we find that the rate of contact between hosts has an ambivalent effect: Dense interaction networks between individuals are considered to facilitate disease outbreaks because of increased pathogen transmission. In social insects, this is compensated by their collective disease defences, i.e., social immunity. For the type of pathogens considered here, we show that even without social immunity, high contact rates between live individuals dilute the pathogen in the host colony and hence can reduce individual pathogen loads below disease-causing levels.

Keywords: epidemiological model | basic reproduction number | obligate killing entomopathogenic fungi | social immunity | biological control

1 Introduction

Obligate killing entomopathogenic fungi like the well-known green muscardine disease (*Metarhizium anisopliae*, Zimmermann (2007)) and white muscardine disease (*Beauveria bassiana*, Barbarin et al. (2012)) are frequently used in biocontrol of pest insects such as, e.g., migratory locusts (Wilson et al., 2002) and mosquitoes (Blanford et al., 2005; Scholte et al., 2005; Thomas and Read, 2007). They are also used against social insects (e.g., termites Almeida et al. (1997) and ants (Jaccoud et al., 1999)), which are particularly successful invasive species (Chapman and Bourke, 2001; Cremer et al., 2008) with a high economic burden (Lowe et al., 2000; Pimentel et al., 2000).

Despite the wide application in biocontrol of the above mentioned entomopathogenic fungi, there is a lack of epidemiological models covering the distinctive features of their particular life history. Specific models are crucial to predict the effects of the use of these fungi as biocontrol agents against pest insects. Most epidemiological models, e.g. the SI model and its extensions, are based on the infection modes typical of diseases such as malaria, influenza, and measles, where the pathogens multiply in the living host such that an increased exposure dose can be spread between individuals.

Obligate killing fungi like *Metarhizium* and *Beauveria*, however, form infectious stages (asexually produced conidiospores) only after having killed their host. These conidiospores can then infect new hosts through direct contact of an insect with an sporulating (infectious) cadaver, or by conidiospores being dispersed and then picked up mostly from the soil around the cadaver. Conidiospores adhere to the insect body surface, germinate, and penetrate the cuticle (Thomas and Read, 2007; Vestergaard et al., 1999). Inside the body, the fungus grows and produces toxins to kill its host. After host death, fungal hyphae and later also a new generation of conidiospores grow out of the dead body.

In addition to picking up the disease from infectious cadavers or from the soil, hosts can

contract the pathogen by contact with other individuals at an early stage after exposure, that carry conidiospores on their body which have not yet strongly adhered to the insect cuticle (Vestergaard et al., 1999) and hence can still be transferred (Konrad et al., 2012). However, there is no multiplication of infectious particles on the surface of a living host, so that contact between two live hosts, at least one of which carries transferable conidiospores on its body, can only lead to a redistribution of the existing conidiospores on both individuals. Thus, transmission via social contact between live hosts leads to a transfer of usually low numbers of infectious particles (Konrad et al., 2012), whereas contraction rates from cadavers are typically very high, at least for ants (Hughes et al., 2004).

Exposure dosage is an important predictor for the likelihood of successful pathogen infection of the host. The entomopathogenic fungi most widely used for biocontrol, *Metarhizium* and *Beauveria*, are host generalists rather than specialists Boomsma et al. (2013). Hence, they require high conidiospore doses for successful host infection (Schmid-Hempel and Frank, 2007). Low-level exposure can lead to micro-infections resulting in a protective immune stimulation rather than disease (Konrad et al., 2012; Rosengaus et al., 1999).

The first aim of our work was therefore to develop a deterministic epidemiological model that accounts for the particular life history of obligate killing entomopathogenic fungi like *Metarhizium* and *Beauveria*. Our model captures their characteristics by deviation from traditional models in a crucial aspect. New infectious particles are brought into the colony by contact with individuals that died from the infection (infectious cadavers). Contact between living hosts does not increase the total number of pathogen particles present in the colony, but simply spreads them between hosts. This means that contact with infectious cadavers leads to a high exposure dose, whereas contact with a live host typically leads to a low exposure dose. As a consequence, we explicitly consider individual host pathogen load by dividing the host colony into multiple exposure classes.

The second aim was to account for host sociality and to include the high interaction

rates among group members as well as their collectively performed sanitary actions. As social insects are characterised by groups of closely related individuals living in high densities and performing frequent social interactions, pathogens would be expected to be easily transmitted across individuals and spread through the host colony Schmid-Hempel (1998). To counteract this risk, social insects have developed a variety of collective disease defence mechanisms, their social immunity (Cremer et al., 2007; Evans and Spivak, 2010; Wilson-Rich et al., 2009), which complement the individual immunity of each group member. One of the most important sanitary behaviours expressed against entomopathogenic fungi is grooming, during which the insects remove infectious particles from the body surface of either themselves (self-grooming) or their nestmates (allogrooming) (Hughes et al., 2002; Rosengaus et al., 1999) and even chemically disinfect them (Tragust et al., 2012). Accordingly, we consider the following factors that influence resistance against pathogens: First, individual immunity comprises hygiene behaviour (e.g., self-grooming) and the immune system of the hosts. Second, social contact may simply denote physical contact or food exchange between individuals. In addition, it can include collective or mutually expressed sanitary actions (e.g., allogrooming) and hence include social immunity into our model. Note that even though we include social features in our model, it can be applied to solitary insects by setting the corresponding parameters to zero.

After model establishment, we derive the conditions under which an entomopathogen can invade a social insect colony. This is done by calculating a basic reproduction number for the pathogen (Heesterbeek, 2002; May et al., 2001). If this number exceeds unity, the disease can spread through the colony; if it is less than one, the colony is protected from disease outbreak. This allows us to determine parameter regimes in which these two scenarios occur. Our result allows for predictions on the evolution of killing rates of obligate killing pathogens. To complete its life cycle, a certain killing rate is necessary for the pathogen to persist. Furthermore, our results show that even in the absence of sanitary

actions, increased contact between individuals is not necessarily to the disadvantage of the host colony.

2 The model

In this section, we set up a model that describes the dynamics between obligate killing pathogens and a social host colony. This model is similar to traditional SI models in dividing the host colony into multiple compartments. The difference to existing, e.g. age structured, models lies within the interactions and transitions between the different compartments. For $x = 0, 1, ..., x_{max}$, let $n_x(t)$ denote the number of hosts carrying pathogen load x at time t. With this notation, n_0 is the class of unexposed individuals and $\{n_1, ..., n_{x_{max}}\}$ can be pooled into what is usually the class of exposed individuals. Useful abbreviations will be $N(t) = \sum_{x=0}^{x_{max}} n_x(t)$ for the total number of live individuals and $\mathbf{n}(t) = (n_x(t))_{x=0}^{x_{max}}$ for the vector displaying the composition of the colony into the classes of different exposure levels. Suppose that the colony is sufficiently large and well mixed in order to use mass action assumptions in the modelling below (i.e., the rate of interactions between two classes x_1 and x_2 is proportional to the product $n_{x_1} \cdot n_{x_2}$, see Hethcote (2000)).

Individual immunity and social interactions: The host dynamics We distinguish between individual immunity and social interactions. Individual immunity summarizes the immune system of each individual, as well as individual sanitary behaviour. Social contact comprises interactions between individuals that may or may not include sanitary actions.

Assume that any given individual undertakes individual immunity measures at rate r_s (for simplicity, let all parameters be independent of exposure level). Then, let a host that carries z conidiospores and performs individual immunity measures have a chance of $0 \leq G_z^x \leq 1$ to end up with x conidiospores. Thus, the individual immunity vectors

$\mathbf{G}^x = (G^x_z)^{x_{max}}_{z=0}$ (for $x = 0, ..., x_{max}$) must have the property $\sum_{x=0}^{x_{max}} G^x_z = 1$ (i.e., the matrix consisting of the $\{\mathbf{G}^1, ..., \mathbf{G}^{x_{max}}\}$ is stochastic) and $G^x_z = 0$ for $x > z$, since pathogen load does not increase by individual immunity.

Let r_c be the rate of social contact between individuals and let S^x_{zy} denote the probability that an individual carrying pathogen load z ends up with pathogen load x given that it has social contact with an individual having pathogen load y. These values are collected into social interaction matrices $\mathbf{S}^x = \left(S^x_{zy}\right)^{x_{max}}_{z,y=0}$ (for $x = 0, ..., x_{max}$) which must fulfil $\sum_{x=0}^{x_{max}} S^x_{yz} = 1$, since the matrices $\mathbf{S}^x$ are probability matrices. Furthermore, total pathogen load must not increase by social contact. As a consequence, $S^x_{zy} = 0$ for $x > z + y$, but this is not sufficient. Note that interactions between hosts always spread the pathogen among individuals (social contact), but only if sanitary actions are taken, it decreases the host colony's total pathogen load.

Including the pathogen The above considerations cover all interactions between the classes n_x, $x = 1, ..., x_{x_{max}}$. The rates at which hosts with pathogen load x die from the pathogen are denoted by the killing rate σ_x, and we collect them in a vector $\boldsymbol{\sigma} = (\sigma_x)^{x_{max}}_{x=0}$. Naturally, the σ_x are increasing in x. By $\nu(t)$, we denote the number of dead individuals. Since obligate killing entomopathogenic fungi proliferate growing out of their hosts' cadavers, $\nu(t)$ gives the number of infectious cadavers that determines the primary exposure risk in the colony. Sporulating cadavers decay at rate η, i.e., their average infectious time is $1/\eta$ time units. This parameter is determined by external biological factors, e.g., weather conditions.

Assuming an unstructured colony, any host may encounter infectious cadavers at rate c per cadaver; that is, each individual is expected to encounter $c\nu(t)$ infectious cadavers per time unit. Usually, infectious cadavers carry huge numbers of infectious particles and thus large amounts of pathogen are transferred upon contact. Therefore, if an individual has

contact with an infectious cadaver, we set its pathogen load to the maximum level x_{max}, independently of its original exposure level.

The differential equation model Assuming that newborns are unexposed, the birth rate $\lambda(\mathbf{n})$ describes the influx of newborns (amount per time unit) into the class n_0. The precise form of $\lambda(\mathbf{n})$ will not be of importance here. Casting all our assumptions into a set of ordinary differential equations gives

$$\dot{n}_x = \lambda(\mathbf{n})\delta_0(x) + c\nu\left(N\delta_{x_{max}}(x) - n_x\right) + \tilde{\mathbf{G}}^x.\mathbf{n} + \frac{r_c}{N}\left(\mathbf{n}.\mathbf{S}^x.\mathbf{n}\right) \tag{1a}$$

$$\dot{\nu} = \boldsymbol{\sigma}.\mathbf{n} - \eta\nu, \tag{1b}$$

where $\tilde{\mathbf{G}}^x = r_s\mathbf{G}^x - (\sigma_x + r_s + r_c)\,\mathbf{e}_{x+1}$ and $\mathbf{e}_i$ denotes the ith unit vector in $\mathbb{R}^{x_{max}+1}$. (The index $i+1$ comes from the fact that we denoted unexposed individuals by n_0, hence the exposure class i is the $(i+1)$th equation of (1a).) The function $\delta_i(x)$ stands for the Kronecker delta function

$$\delta_i(x) = \begin{cases} 1 & : x = i \\ 0 & : x \neq i \end{cases}.$$

An overview of the parameters is given in Table 1.

Interpretation of equation (1b) is straightforward: The number of hosts dying from the pathogen each time unit is $\boldsymbol{\sigma}.\mathbf{n}(t) = \sum_{x=0}^{x_{max}} \sigma_x n_x(t)$, and the decay of cadavers is given by $\eta\nu(t)$. Note that no natural death of hosts is included in the model. The structure of equation (1a) is explained as follows. The first term on the right hand side of equation (1a) gives the influx of newborn individuals; it only appears if $x = 0$. The second term describes the effect of new exposures. Upon contact with infectious cadavers, individuals are removed from their class ($-c\nu n_x$) and added to the class of maximal exposure level ($c\nu N\delta_{x_{max}}$). The third term, $\tilde{\mathbf{G}}^x.\mathbf{n}$, describes the remaining linear interactions. Individuals are removed from

λ	...	birth rate	r_c	...	contact rate
c	...	rate of encountering an infectious cadaver	r_s	...	rate of performing individual immunity measures
$\boldsymbol{\sigma}$	...	vector of σ_x, the rates of dying from the pathogen	S^x_{zy}	...	probability of $z \mapsto x$ upon contact with y
η	...	rate of decay of cadavers	G^x_z	...	probability of $z \mapsto x$ by means of individual immunity

Table 1: Overview of parameters.

exposure class x if they die, perform individual immunity measures, or enter social contact ($-(\sigma_x + r_s + r_c)n_x$), and they enter it if starting out in a higher class and losing enough conidiospores by individual immunity measures ($r_s \mathbf{G}^x.\mathbf{n}$). The last (quadratic) term in equation (1a) comprises all pairwise interactions that add individuals to exposure class x due to contact between hosts, possibly including sanitary actions. Note that in the model (1) no variable can become negative, given non-negative starting conditions. Furthermore, with no hosts or no pathogen initially, neither hosts nor pathogen will emerge *de novo*.

3 Results

Our results are mostly concerned with identifying conditions under which a healthy colony is able to resist the invasion of a pathogen. We assume a healthy colony that has equilibrated at a steady state, which we denote by a pathogen-free equilibrium $\mathbf{E}$. If a small amount of pathogen (e.g., a single infectious cadaver) is introduced, the colony can either successfully drive out the pathogen, or the disease is able to spread. In the first case, we say that the colony is protected from the pathogen, in the latter we speak of the outbreak of the disease. Mathematically, this corresponds to evaluating the stability of the pathogen-free equilibrium: If the pathogen-free equilibrium $\mathbf{E}$ is asymptotically stable, the dynamics (1) will converge back to $\mathbf{E}$ under small perturbations, hence the colony is protected from the pathogen. The following Section 3.1 considers the simplest possible exposure class archi-

tecture. In Section 3.1.1, a condition for asymptotic stability of **E** is derived in terms of a basic reproduction number $\tilde{R}_0$. Section 3.1.2 provides a technical comment that puts $\tilde{R}_0$ in mathematical context, and Section 3.1.3 discusses the implications of successful pathogen invasion. Finally, Section 3.2 relaxes the stringent assumptions of Section 3.1. Permitting more general exposure class structures, we extend our analytic results using numerical simulations and show in which area of the parameter space the colony is protected from the pathogen.

3.1 Analytical results

3.1.1 Invasion of the pathogen

Consider the following case: There are only three classes of pathogen load, i.e., we distinguish between unexposed ($x = 0$), lightly exposed ($x = 1$), and severely exposed ($x = 2$) hosts. By setting $\sigma_0 = \sigma_1 = 0$ and $\sigma_2 = \bar{\sigma} > 0$, we make sure that only hosts that carry a large pathogen load die from the pathogen. With no pathogen present (i.e., $n_1 = n_2 = \nu = 0$), the host colony will evolve according to $\dot{n}_0(t) = \lambda(\mathbf{n})$. For any positive stable fixed point of $\dot{n}_0(t) = \lambda(\{n_0(t), 0, 0\})$, i.e., $\lambda(\{K, 0, 0\}) = 0$ for $K > 0$, we can define a pathogen-free equilibrium, **E**, by

$$n_0 = K,\ n_1 = n_2 = \nu = 0.$$

Since **E** is assumed to be a stable equilibrium of the healthy colony, we have $\frac{\partial \lambda}{\partial n_0}|_{\mathbf{E}} < 0$.

Upon linearisation of the equations (1) at the pathogen-free equilibrium with the above

simplifications, we obtain the Jacobian

$$\mathbf{J} = \begin{pmatrix} \frac{\partial \lambda}{\partial n_0}|_{\mathbf{E}} & * & * & cK \\ 0 & -\Lambda & * & 0 \\ 0 & 0 & -\zeta - \bar{\sigma} & cK \\ 0 & 0 & \bar{\sigma} & -\eta \end{pmatrix} \tag{2}$$

(the order of the variables is $\{n_0, n_1, n_2, \nu\}$), where the asterisks comprise information about individual and social immunity efficiency that is not relevant for the investigations to follow, and

$$\Lambda = r_c \left(1 - \left(S_{01}^1 + S_{10}^1\right)\right) + r_s \left(1 - G_1^1\right),$$
$$\zeta = r_c \left(1 - \left(S_{02}^2 + S_{20}^2\right)\right) + r_s \left(1 - G_2^2\right).$$

The terms Λ and ζ are positive Before proceeding, we argue that Λ and ζ are positive. Both Λ and ζ reflect the host colony's innate ability to reduce its pathogen load or spread pathogens between individuals. As stated in Section 2, social interactions and individual immunity do not increase the total pathogen load in the host colony. Thus, we must exclude the case that, e.g., a healthy individual meets a heavily exposed individual and becomes exposed without changing the state of its contact partner. In other words, the probability that the healthy host becomes heavily exposed can be at most the probability that the other individual does not stay heavily exposed, i.e., $S_{02}^2 \leq 1 - S_{20}^2$. Therefore, we get $S_{02}^2 + S_{20}^2 \leq 1$ and, for the same reason, $S_{01}^1 + S_{10}^1 \leq 1$. Since the G_z^x are probabilities, it follows that $\Lambda \geq 0$ and $\zeta \geq 0$.

The magnitude of Λ displays the effectiveness in curing lightly exposed individuals. Since a slight exposure does not entail the risk of dying in this simplistic model, the value of Λ has no qualitative influence on the invasion condition (as long as Λ is truly positive).

The interesting quantity is ζ, which measures the propensity to get individuals out of the critical exposure class.

The basic reproduction number For the pathogen-free equilibrium to be asymptotically stable (i.e., a small amount of pathogen cannot destabilize the colony), we require all four eigenvalues of $\mathbf{J}$ to have negative real parts — if just one eigenvalue has positive real part, the equilibrium is unstable and the slightest amount of pathogen will lead to a outbreak of the disease. Due to the simple structure of $\mathbf{J}$, its first two eigenvalues, $\frac{\partial\lambda}{\partial n_0}|_{\mathbf{E}}$ and $-\Lambda$, can be read directly from its diagonal. As stated above, $\frac{\partial\lambda}{\partial n_0}|_{\mathbf{E}}$ and $-\Lambda$ are negative. Thus, we can focus on the two remaining eigenvalues, which are contained in the 2×2-submatrix

$$\begin{pmatrix} -\zeta - \bar{\sigma} & cK \\ \bar{\sigma} & -\eta \end{pmatrix}.$$

Directly evaluating negativity of the eigenvalues of this matrix is relatively intricate, but applying the Routh-Hurwitz criterion (Hurwitz, 1895; Routh, 1877) produces a very simple condition for the stability of the system: The remaining eigenvalues have negative real parts if

$$1 > \frac{\bar{\sigma}}{\zeta}\left(\frac{cK}{\eta} - 1\right). \tag{3}$$

Equivalently, in tradition of theoretical epidemiology, this can be written as a basic reproduction number,

$$\tilde{R}_0 = \frac{cK}{\eta}\frac{\bar{\sigma}}{\bar{\sigma} + \zeta}. \tag{4}$$

Thus, if $\tilde{R}_0 < 1$, the pathogen-free equilibrium is asymptotically stable and the colony is protected from pathogen invasions. Conversely, $\tilde{R}_0 > 1$ means that the pathogen successfully enters the colony. Note that $\tilde{R}_0$ takes the same form for $x_{max} > 2$ if $\sigma_x = 0$ for $x < x_{max}$.

Formally, calling $\tilde{R}_0$ a basic reproduction number is not perfectly correct, since the formal derivation of R_0 produces a slightly different result. We added a tilde in equation (4) to symbolize the distinction from the strict mathematical definition of the basic reproduction number R_0. In the following section, Section 3.1.2, we argue that the difference between R_0 and $\tilde{R}_0$ it is irrelevant in the present case. Verbally, we keep denoting $\tilde{R}_0$ by the basic reproduction number of the pathogen for the sake of simplicity.

Upon closer examination of (4), the structure of $\tilde{R}_0$ provides interesting insight. It separates the efficiency of primary exposures from infectious cadavers and the effectiveness with which the pathogen kills its host. For the pathogen to be able to invade, it is necessary that, on average, each infectious cadaver kills at least one host. This is reflected in $\tilde{R}_0$, which is the product of net infection rate, cK/η, times the probability that a host does not recover from the pathogen, $\bar{\sigma}/(\bar{\sigma}+\zeta)$. Since the latter is bounded by one, the total exposure rate, cK, needs to exceed the decay rate of cadavers, η. Furthermore, a high killing rate $\bar{\sigma}$ increases the value of R_0, which can be counteracted by an efficient (social) immune system described by ζ.

Note that even without individual and social immunity, i.e., with social contact alone, ζ is positive. Hence, the propensity to quickly spread the pathogen in the colony has a similar effect as the actual removal of infectious particles. This will be made clearer in Section 3.2.

3.1.2 A technical comment on $\tilde{R}_0$

The basic reproduction number R_0 is defined as the expected number of secondary infections caused by a single primary infection in a susceptible colony. Diekmann et al. (2010) provide a procedure for calculating the basic reproduction number for any compartmental model as the spectral radius of the "next-generation matrix" $\mathbf{K}$. Following their procedure

to construct $\mathbf{K}$ shows that its spectral radius is

$$R_0 = \max\left\{\frac{r_c S_{0,1}^1}{\Lambda + r_c S_{0,1}^1}, \frac{cK\bar{\sigma} + r_c\eta S_{0,2}^2}{\eta\left(\bar{\sigma} + \zeta + r_c S_{0,2}^2\right)}\right\}. \tag{5}$$

First and most importantly, this expression and our definition of $\tilde{R}_0$ in equation (4) produce the same critical threshold between invasion and extinction of the pathogen. Second, it is worth noting that the first argument of the *max* function in equation (5) can be greater than the second (e.g. if η is large and Λ is small). However, in this case none of the two arguments can be greater than unity. Third, assuming $S_{0,2}^2 = 0$ can be justified since it corresponds to an unexposed individual picking up all the pathogens of its heavily exposed interaction partner. Thus, the two hosts swap infection classes without a net effect on the state of the system. With this additional specification, the second argument of the *max* function equals our definition of $\tilde{R}_0$. Overall, we hence stick to the relatively simple expression of equation (4), referring to $\tilde{R}_0$ as the basic reproduction number for our system.

3.1.3 The endemic equilibrium

If $\tilde{R}_0 > 1$, the pathogen can invade the host colony and the system becomes endemic. In theory, equations (1) can be solved explicitly for endemic equilibria with the specifications of this section, see Section 3.1.1. However, the complexity of the resulting analytic expressions prevents a deeper understanding of the system. Numerical simulations, however, suggest that whenever $\tilde{R}_0 > 1$, the dynamics converge to a unique, globally stable endemic equilibrium solution.

How much does a small amount of pathogen impact a healthy host society and how does it scale with increasing basic reproduction number $\tilde{R}_0$? To answer this question, we performed numerical simulations without the recruitment of newborn hosts (i.e., $\lambda \equiv 0$). The reduction in colony size after the system equilibrates is a measure for the impact of the

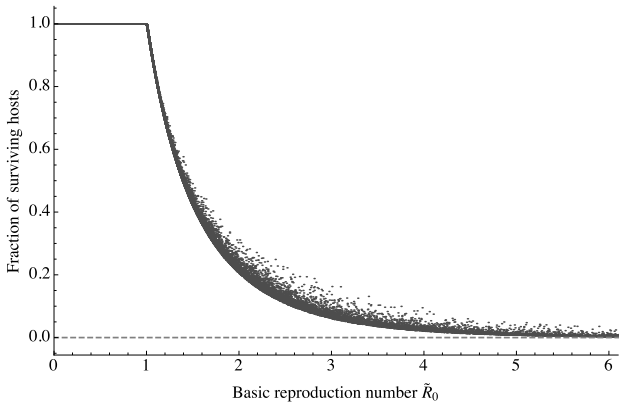

Figure 1: The fraction of surviving hosts after a pathogen invasion. To obtain each of the 100,000 data points, values for c, η, and $\bar{\sigma}$ were drawn randomly from a uniform distribution on $[0, 1]$. Then, $\tilde{R}_0$ was evaluated and the dynamics following pathogen invasion were simulated until they reached their equilibrium. For $\tilde{R}_0 < 1$, the size of the host colony remains virtually unchanged. Above the threshold $\tilde{R}_0 > 1$, the fraction of surviving hosts decreases approximately exponentially. The individual data points do not lie on a single curve, hence the exact parameter composition rather than $\tilde{R}_0$ alone matter for the result. The remaining parameter values are $\lambda \equiv 0$, $r_c = r_s = 1$, and $K = 1$. S^x_{zy} and G^x_z were specified such that $\zeta = 0.2$.

pathogen. Clearly, there can be only two possible outcomes in the absence of births: Either, the pathogen eradicates the host colony and thus dies out itself, or the pathogen becomes extinct first and leaves a healthy colony of reduced size. Our simulation results, depicted in Figure 1, show that the latter is always the case in our deterministic model. As the size of the colony decreases in the course of a simulation, the number of new primary infections is reduced. Eventually, this number of new infections does not sustain the persistence of the pathogen, such that it is cleared from the host colony.

As Figure 1 clearly shows, the decline in colony size, and hence the impact of the pathogen, is largely determined by the value of $\tilde{R}_0$. We observe an approximately exponential reduction of colony size once the basic reproduction number exceeds its threshold $\tilde{R}_0 = 1$. However, the impact of the pathogen is not solely determined by $\tilde{R}_0$, but depends on the individual parameters in the model, see Figure 1.

3.2 Higher numbers of exposure classes

The result of the previous section has been derived under very rigid assumptions. As soon as more than one class of exposed hosts can die from the pathogen, analytical investigations analogously to those in Section 3.1 become infeasible. With the following simulations, we aim to relax the preconditions on the number of exposure classes to $x_{max} > 2$ and indicate that an invasion condition similar to (3) holds in more general cases.

Specifications Suppose that there is some critical pathogen load x_{crit}, the infective dose, above of which hosts die at constant rate $\bar{\sigma}$. As long as the threshold $\bar{\sigma}$ is not exceeded, hosts do not die from the pathogen. In short, this means

$$\sigma_x = \begin{cases} 0 & : x \leq x_{crit} \\ \bar{\sigma} & : x > x_{crit} \end{cases} .$$

To simulate the model (1), we specify $\mathbf{G}^x$ by equation (A.1), $\mathbf{S}^x$ by equation (A.4) in A. The former, equation (A.1), is given by a binomial distribution where exposure classes are reduced independently. The latter, equation (A.4), describes the redistribution of spore classes between the two interacting individuals, on top of which spore classes can be lost by allogrooming. The rather cumbersome rule for $\mathbf{S}^x$ ensures that exposure loads do not fall below zero or exceed x_{max}. The growth rate $\lambda(\mathbf{n})$ follows a logistic growth model. Furthermore, we set $x_{max} = 10$ and $x_{crit} = x_{max}/2 = 5$. This particular exposure class architecture, $x_{crit} = x_{max}/2$, will be relaxed below.

Initially, the host colony is assumed to be unexposed at its pathogen-free equilibrium $\mathbf{E}$ (given by $n_0(0) = K$, $n_x(0) = 0$ for $0 < x \leq x_{max}$, $\nu = 0$). The effect of a small perturbation away from $\mathbf{E}$ is investigated by numerically evaluating the Jacobian of system (1) to test if the pathogen-free equilibrium is stable. This reveals the transition in parameter space between the pathogen being cleared out of the colony and being able to persist in the long

run. Invoking the notion of the basic reproduction number, this transition is given by $R_0 = 1$.

Comparison with the analytic result Figure 2 shows the simulation results of the area in which the pathogen can invade the host colony depending on the total rate of cadaver contact, cK, and the decay rate of cadavers, η, for various configurations of the remaining parameters. Within the light grey area, the host colony is protected from the pathogen, whereas in the dark area it is not. In concordance with the linear relationship between cK and η in $\tilde{R}_0$, see equation (4), these regions are separated by a straight line; the slope of the line decreases with increasing $\bar{\sigma}$. Notably, even for high killing rates $\bar{\sigma}$ and small defence parameters, the line never drops below the diagonal $cK = \eta$. Hence, it is given by $cK = \eta(1 + k)$ for some $k > 0$, which is a function of $\bar{\sigma}$ and the remaining parameters. Rearranging terms produces

$$1 = \frac{cK}{\eta} \frac{1}{1+k}. \tag{6}$$

In the simplistic case of Section 3.1 leading to equation (4), we have $k = \zeta/\bar{\sigma}$, but evaluating k for several values of $\bar{\sigma}$ reveals that its structure is more complicated in the general case. For large $\bar{\sigma}$ or weak defensive mechanisms of the host (small ζ in the above diction), k converges to zero. However, its exact form depends on the details of the model and is hard to determine. In particular, $1/k$ is not linear in $\bar{\sigma}$ in general.

Simulations depicted in Figure 3 show the invasion ability of the pathogen in dependence on $\bar{\sigma}$ and the relative exposure rate $\alpha = cK/\eta$. This compound parameter measures the overall rate of primary exposures (cK) relative to the decay rate of infectious cadavers. Clearly, increasing the hosts' defensive mechanisms (e.g. by increasing r_c and r_s) enlarges the area in which the host colony is protected from pathogen invasion (Figures 3a and 3b). The same pattern is observed when increasing only the rate of contact between individuals,

r_c, in the absence of immune defence mechanisms, i.e., if $G_z^x = 0$ for $x \neq z$ and $S_{zy}^x = 0$ for $x \neq y + z$ (Figures 3c and 3d). Hence, as predicted from the structure of ζ in a previous section, Section 3.1.1, increased contact between host individuals increases the basic reproduction number and hence hinders pathogen invasion in this scenario.

In the case of equation (4), $\tilde{R}_0 = 1$ shows a hyperbolic dependence between α and $\bar{\sigma}$. According to the above finding that $1/k$ is non-linear in $\bar{\sigma}$, the separation between the areas of pathogen invasion and the colony being protected is not a perfect hyperbola in Figure 3. However, varying c, K, and $\bar{\sigma}$ such that α remains constant leaves the numerical results unchanged. Hence, these parameters indeed enter $\tilde{R}_0$ only through the combination cK/η.

Overall, our simulations demonstrate that the essential structure of the basic reproduction number (4) is maintained in more general cases than treated in Section 3.1. In particular, if the pathogen can invade, the exposure rate from infectious cadavers must exceed their decay rate ($cK > \eta$), i.e., infectious cadavers expose on average more than one host to the pathogen during their infectious period. Furthermore, $\tilde{R}_0$ increases with $\bar{\sigma}$, hence a high killing rate is to the benefit of the pathogen.

The infective dose x_{crit} Both our analytical results and the simulation results above were obtained for a particular exposure class architecture, $x_{crit} = x_{max}/2$. This choice of the infective dose x_{crit}, however, is at a threshold for more complicated behaviour. While $x_{crit} > x_{max}/2$ qualitatively leads to the same results $x_{crit} = x_{max}/2$ (simulations not shown), the picture is different for $x_{crit} < x_{max}/2$. The reason for this phenomenon is explained as follows: If the infective dose is above the threshold of $x_{max}/2$, a single exposure to an infectious cadaver does not have the potential to kill more than one host. Therefore, from the perspective of the pathogen, infectious particles should exhibit high killing rates $\bar{\sigma}$ to prevent being diluted in the colony and ensure the death of the primarily

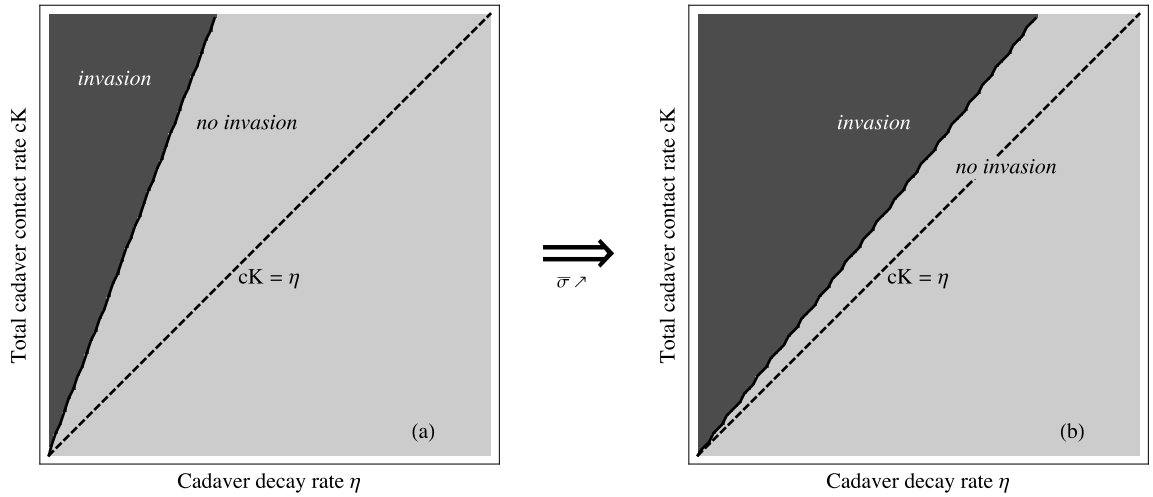

Figure 2: Stability of the pathogen-free equilibrium in the η-cK-plane with increasing $\bar{\sigma}$. In the light grey area, the colony is protected from the pathogen, while in the dark area, the pathogen can invade. These areas are separated by a straight line. Its slope decreases with increasing $\bar{\sigma}$, enlarging the dark grey area. Hence, a high killing rate increases the ability of the pathogen to invade the host colony. However, the separating line never drops below the diagonal $cK = \eta$. Thus, cadaver contact must occur at a minimal threshold rate even if the killing rate is high. The slope of the separating line gradually decreases as $\bar{\sigma}$ increases from (a) 0.25 to (b) 1.0 (intermediate values are not shown). The remaining parameters are $r_c = r_s = 1$, $x_{max} = 10$, and $x_{crit} = 5$. Consult the appendix for the specifications of λ, S^x_{zy} and G^x_z. Values of cK and η range from 0 to 5 at a resolution of 100 points.

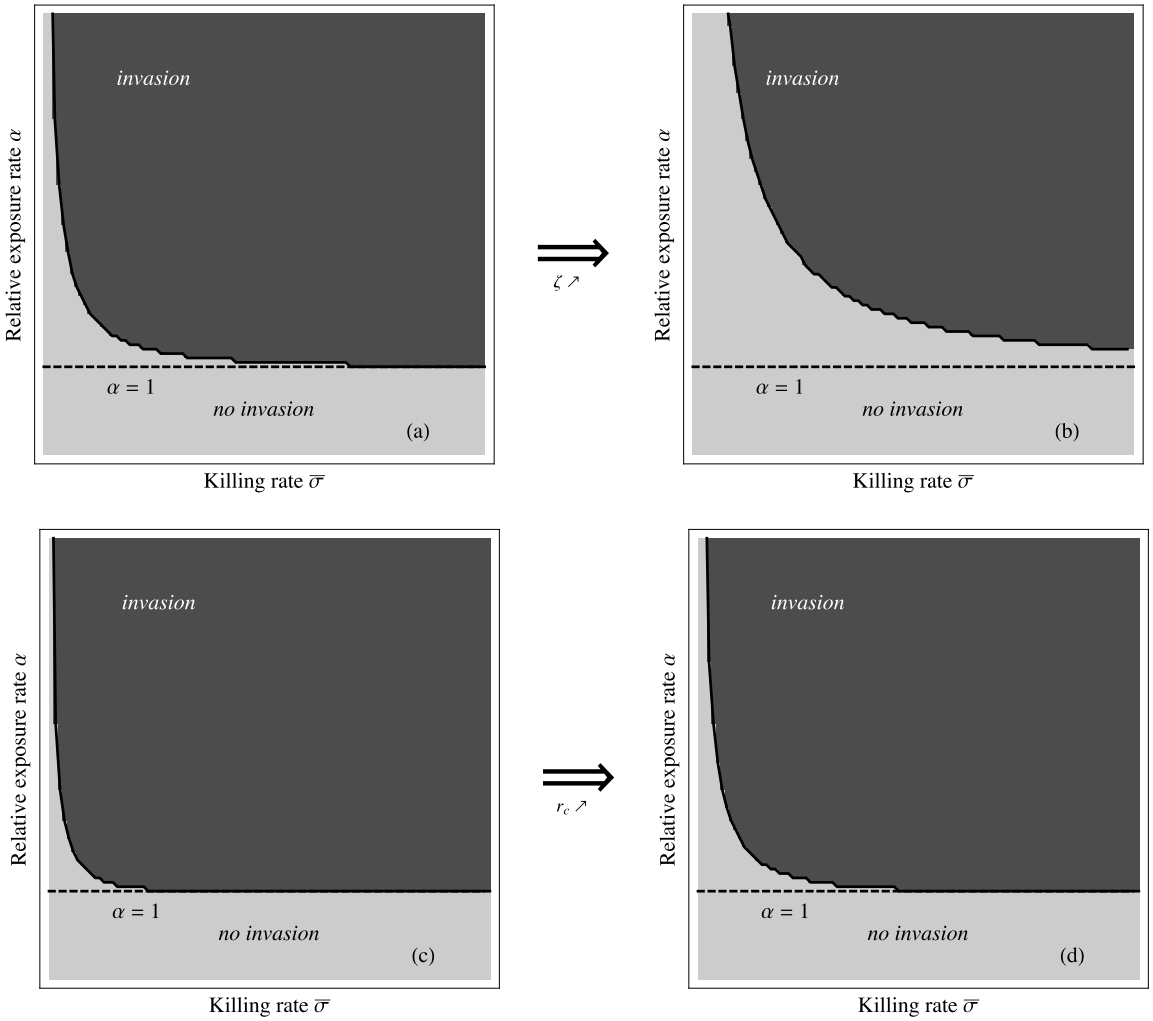

Figure 3: Stability of the pathogen-free equilibrium in the $\bar{\sigma}$-α-plane, where $\alpha = cK/\eta$, with increasing contact rate r_c and individual immunity rate r_s: In the light grey area, the colony is protected from the pathogen, while in the dark area, the pathogen can invade. High killing rate $\bar{\sigma}$ decreases the threshold for pathogen invasion on α to a minimal value of $\alpha = 1$, i.e., $cK = \eta$ (compare Figure 2). We increase the host's immune defence mechanisms by increasing r_c and r_s simultaneously from (a) 1.0 to (b) 4.0. As expected, this leads to a larger area in which the colony is protected from the pathogen by increasing the threshold on α. Similarly, the area of protection grows if we assume no immune defence mechanisms ($G_z^x = 0$ for $x \neq z$ and $S_{zy}^x = 0$ for $x \neq y + z$) and increase r_c alone from (c) 2.0 to (d) 4.0. The variables $\bar{\sigma}$ and α range from 0 to 5 at a resolution of 100 points and the remaining parameters are specified as in Figure 2.

exposed host. Contrariwise, if the infective dose is low, $x_{crit} < x_{max}/2$, interactions between hosts following a single initial exposure can lead to more than one individual exceeding the infective dose. Accordingly, there is an optimal killing rate $\bar{\sigma}_{opt}$ for the pathogen in the sense that it maximizes the area in which it can invade. This optimal value trades off the ability of the pathogen to kill its host with the chance to cause secondary infections.

The existence of an optimal killing rate is shown in Figure 4a. The threshold $\tilde{R}_0 = 1$ that separates the region where the pathogen invades the host colony from the region where the host colony is protected from the pathogen now clearly extends below $\alpha = 1$. At its minimum is the optimal killing rate for the pathogen, $\bar{\sigma}_{opt}$. This shows that even if infectious cadavers on average cause less than one primary exposure, a pathogen with adjusted killing rate may be able to invade the colony, since the number of critical secondary exposures can compensate for the low transmission rate from cadavers. Note that for large killing rate $\bar{\sigma}$, the threshold $\tilde{R}_0 = 1$ again converges towards $\alpha = 1$, i.e., towards one exposure per infectious cadaver on average. Hence, if hosts die from the pathogen before being able to spread infectious particles, only a positive net primary exposure rate matters for the success of the pathogen.

Further simulations with low infective dose x_{crit} reveal an ambivalent effect of high contact between individuals. A change of contact rates between individuals, r_c, lowers the threshold in some parameter domains and increases it in others. If the killing rate is above its optimal level $\bar{\sigma}_{opt}$, hosts die before the optimal pathogen spread is reached. In this case, a denser contact network facilitates pathogen spread and thus makes invasion into the colony easier for the pathogen. Conversely, if the killing rate is below its optimal level, increased contact rates raise the invasion threshold for the pathogen, making pathogen invasion into the colony more difficult by diluting pathogen dose. This can be seen comparing Figure 4b with Figure 4a: As the contact rate between individuals (r_c) increases, the optimal killing rate $\bar{\sigma}_{opt}$ shifts to the right. Left of $\bar{\sigma}_{opt}$, the threshold for pathogen invasion is raised, while

to its right it is lowered.

In the case of $x_{crit} \geq x_{max}/2$ above, we found a simple sufficient condition for the colony being protected from pathogen invasion in terms of pathogen transmission rates from infectious cadavers; if $\alpha < 1$, the colony was protected independently of the other parameters. Here, if $x_{crit} < x_{max}/2$, the existence of such a threshold remains valid but its value may change. There is a positive relative exposure rate, α_{min} in Figure 4a, below which the host colony is sure to be protected from pathogen invasions. This threshold depends on the architecture of exposure classes, i.e., on x_{crit} and x_{max}. It displays the minimal rate of primary exposures from infectious cadavers necessary for the outbreak of the disease, given that the killing rate is adjusted optimally to the realities. Note that in both cases, $x_{crit} < x_{max}/2$ and $x_{crit} \geq x_{max}/2$, the parameters c, K, and η enter the invasion condition only through the combined parameter $\alpha = cK/\eta$. That is, changing their values such that α remains constant did not change the invasion condition in any of our simulations.

4 Discussion

We present an epidemiological model for a pathogen that does not replicate on the living host, but kills the host before setting free the next generation of infectious particles. This occurs, e.g., in the obligate killing entomopathogenic fungi *Metarhizium* and *Beauveria*. For these pathogens, the total number of infectious particles present in the host colony – like that of insect societies, which remove their dead from the nest – can only be increased by bringing them in from outside the colony, mostly by foraging individuals getting exposed by contact to infectious cadavers. Contact between living hosts only leads to redistribution of infectious particles, whereby a reduction in pathogen load of one individual is linked to the equivalent increase of pathogen load in the interacting individual.

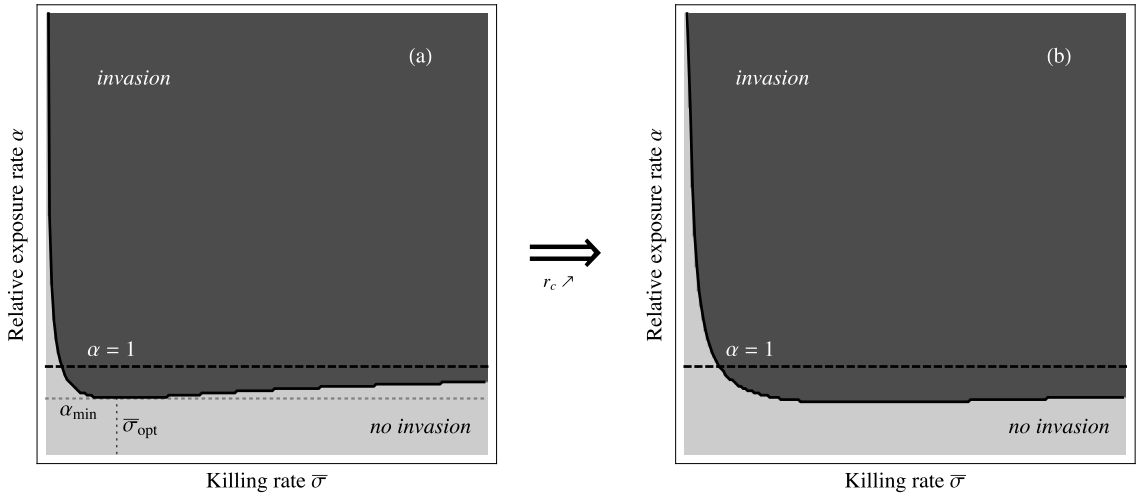

Figure 4: Stability of the pathogen-free equilibrium in the $\bar{\sigma}$-α-plane, where $\alpha = cK/\eta$, for low infective dose, $x_{crit} = x_{max}/5 = 2$. In the light grey area, the colony is protected from the pathogen, while in the dark area, the pathogen can invade. (a) The drop of the separating line between these areas below $\alpha = 1$ gives rise to an optimal killing rate for the pathogen, $\bar{\sigma}_{opt}$. If α is lower than a threshold α_{min}, the host colony is protected from pathogen invasion independent of the other parameters. (b) Increasing the rate of contact between individuals, r_c, shifts the optimal killing rate $\bar{\sigma}_{opt}$ to the right. Thereby, it raises the threshold for pathogen invasion to the left and increases it the right of $\bar{\sigma}_{opt}$. For parameter values, confer A.2.

While no increase in the number of infectious particles can occur inside the colony, hosts can actively reduce the pathogen load by active behavioural defences, such as individual self- and social allogrooming. Group living can thus reduce the individual risk of infection through reduction of the exposure dose by (i) the dilution effect caused by a redistribution of infectious particles through social contact (in the absence of social immunity) and (ii) an additional mechanical removal and/or chemical disinfection of infectious particles by active host defences. We study the ability of such a pathogen to invade a colony of social insect hosts.

To consider varying exposure levels and dose-dependent killing rates, our model groups hosts into several exposure classes. The exposure class architecture is determined by the number of exposure classes, x_{max}, and a infective dose, x_{crit}. The former determines the resolution of exposure differences between hosts and sets a scale for the rates at which hosts traverse between classes (S^x_{zy} and G^x_z). These rates directly influence individual and social host defences and hence have an effect on the host-pathogen dynamics that are independent of the other parameters. Our qualitative results, however, are independent of the specific choice of x_{max}.

Pathogen-induced mortality is typically a sigmoidal function that connects a baseline value for no pathogen exposure with doses inflicting maximal mortality, as determined in several laboratory-based studies (Hughes et al., 2004; Milutinović et al., 2013; Vestergaard et al., 1995). In principle, our model can capture any form of dose-dependent mortality by assigning a killing rate σ_x to every exposure class x. Here, we chose a threshold-type of dose dependence that assumes a critical exposure class x_{crit}, where the killing rate switches from zero to a constant positive value $\bar{\sigma}$. This is a simplification of natural conditions that is only justified if mortality induction changes sufficiently abruptly, which seems valid in our *Metarhizium*-and model system (Hughes et al., 2004), but has to be evaluated for each particular host-pathogen system. Simulations with gradually increasing $\bar{\sigma}$ (not shown)

indicate that our qualitative results fully apply if x_{crit} is considered the lowest exposure class for which σ_x is positive. Moreover, using such threshold-type dose dependence involves that the choice of x_{crit} has quantitative implications on the dynamics. Yet, the qualitative pattern of the invasion condition for the pathogen only changes as x_{crit} falls below $x_{max}/2$ (see below).

Our analysis rests on the concept of the basic reproduction number, R_0, to determine the ability of the pathogen to invade a healthy host colony (Heesterbeek, 2002): If $R_0 < 1$, the host colony is protected from the pathogen, whereas the disease breaks out if $R_0 > 1$. For many pathogens, the basic reproduction number can be written as the product of the infection rate and the average duration of infectiousness of hosts (May et al., 2001). Here, we find a similar separation for the basic reproduction number of our system, $\tilde{R}_0$: It is the product of the relative rate of primary exposures, $\alpha = cK/\eta$, and the probability of a host dying from the pathogen, $\bar{\sigma}/(\bar{\sigma} + \zeta)$, see equation (4).

If the basic reproduction number exceeds unity, the pathogen can invade the host colony and an endemic equilibrium is attained. The impact of the pathogen on the host colony can be measured in terms of the reduction in colony size following a pathogen invasion. We find that the impact of the pathogen on the host colony scales approximately exponentially with the basic reproduction number, see Figure 1. Hence, the basic reproduction number is a meaningful proxy for the long-term consequences of an outbreak of the disease. Notably, however, the pathogen never eradicates the host colony in our model, even if there is no recruitment of newborn hosts.

Focussing on conditions for pathogen invasion, we find that individual and social host defences are effective against the invasion of obligate killing entomopathogenic fungi into the colony. Elevated individual and social immunity or increased contact rates increase the parameter ζ in equation (4) and hence reduce the basic reproduction number. Figure 3 shows that this diminishes the region of pathogen invasion by imposing stronger conditions

on the remaining parameters. We made similar observations in the simulations leading to Figures 2 and 4.

From the expression of the basic reproduction number, equation (4), we furthermore see that $\tilde{R}_0$ cannot exceed unity if the rate of contact with infectious cadavers, cK, is below the cadaver decay rate η. In the setting of our simulations (Section 3.2), the same holds true if $x_{crit} \geq x_{max}/2$, i.e., if being in the lower half of exposure classes does not entail the risk of dying from the pathogen. This is reflected by Figure 2: Below the diagonal, i.e., if $cK < \eta$, the host colony is always protected from pathogen invasion, independent of the other parameters, i.e., $\bar{\sigma}$ and the parameters contained in ζ. Equivalently, in Figure 3 the area of invasion never extends below $\alpha = cK/\eta = 1$. If $x_{crit} \leq x_{max}/2$, we still find a minimal value $\alpha_{min} > 0$, that depends on x_{crit} and x_{max}, such that the area of invasion never extends below α_{min} (see Figure 4). Overall, this shows that the transmission rates from infectious cadavers need to exceed a threshold set by the duration of infectiousness of infectious cadavers and the relation between the average amount of pathogen transmitted from infectious cadavers and the infective dose given by x_{max} and x_{crit}.

The basic reproduction number $\tilde{R}_0$ in equation (4) furthermore indicates that the success of the pathogen is basically determined by the product of the efficiency of causing new exposures and the probability of the host dying from the pathogen. Hence, high killing rates should increase the probability of pathogen invasion. In particular, Figure 2 shows that increased killing rates enlarge the region in which the disease breaks out. However, this is due to the choice of the infective dose as $x_{crit} \geq x_{max}/2$. With this specification, no more than one host can exceed the critical pathogen level from a single primary exposure. Hence, from the perspective of the pathogen, the dilution of its infectious particles through redistribution among hosts between individuals is detrimental, therefore selecting for a higher killing rate or lower infective dose to assure host killing. Yet, if the infective dose is low compared to the maximum pathogen load, $x_{crit} < x_{max}/2$, secondary exposures

from a primarily exposed host potentially exceed the infective dose. Therefore, an intermediate killing rate, $\bar{\sigma}_{opt}$, is optimal for the pathogen (see Figure 4); it arises from the tradeoff between the chance of critically exposing multiple hosts and the pathogen's ability to ensure the killing of its hosts before its pathogen load on individual hosts drops too low.

To study the effect of the density of the contact network in the host colony, we can fix immune defence parameters and vary the rate of contact, r_c. Since the parameter ζ in the basic reproduction number $\tilde{R}_0$ increases with contact rate r_c, increased contact rates have an effect similar to increased immunity and hence reduce $\tilde{R}_0$. In the case of low infective dose, however, our numerical simulations indicate that this is only true if the killing rate of the pathogen is below its optimum, $\bar{\sigma}_{opt}$ (see Figure 4). In the other case, $\bar{\sigma} > \bar{\sigma}_{opt}$, increased contact rates lower the basic reproduction number and hence facilitate disease spread. Note that any effect of the contact rates between hosts on the basic reproduction number is a dilution effect that spreads pathogen load between hosts. It can have a similar effect as, but should not be confused with mechanisms of individual or social immunity.

These findings lead to our main conclusions. First, social immunity is an effective mechanism to prevent disease outbreaks in host societies. This is not surprising given the sophisticated collective behaviours described in empirical studies of social insects (reviewed by Cremer et al. (2007); Evans and Spivak (2010); Wilson-Rich et al. (2009)). However, social immunity is contained in our parameter ζ, which also includes individual immunity and the dilution of pathogens due to physical contact between individuals. Hence, in our model, social and individual immunity feed into the same quantity ζ and thus complement each other in an overall immunity. Therefore, our remaining results also apply to host species without social immune defence mechanisms. They are not specific to social species but consequences of the particular life history of the obligate killing pathogens studied here.

Second, successful invasion of the pathogen is determined by two factors: successful

infection and killing of the host. This is in close analogy to the most common models of disease dynamics, where the basic reproduction number can be written as a product of the infection rate and the average duration of infectiousness (May et al., 2001). Concerning successful host infection, we find a minimal pathogen transmission rate required for pathogen invasion. If the total infective rate per infectious cadaver, cK, relative to its decay rate, η, is below the threshold $cK/\eta = \alpha_{min}$, the pathogen cannot invade the host colony independently of the other parameters (i.e., $\bar{\sigma}$, r_c, r_s, $\mathbf{S}^x$, $\mathbf{G}^x$). The value of α_{min} depends on the exposure class architecture described by x_{crit} and x_{max}. More precisely, the critical exposure threshold (i.e. the infective dose), above which the pathogen becomes lethal for its host, determines the minimal number of primary exposures one infectious cadaver must cause on average. For example, if contact between a single host and an infectious cadaver transfers just enough pathogenic particles to bring the host above the infective dose ($x_{crit} \geq x_{max}/2$), a cadaver must, on average before decaying, expose (and reliably kill) more than one host for the disease to break out. Lower infective doses make it possible that the minimal exposure rate from infectious cadavers, α_{min}, is below one, since one primary exposure has the potential to cause several hosts deaths.

The second factor for successful invasion of the pathogen is its ability to kill its host. Thus, it is not surprising that obligate killing pathogens require substantial killing rates. This is confirmed by our model: If the infective dose is at least half the maximal exposure level ($x_{crit} \geq x_{max}/2$), an increasing killing rate always decreases the threshold of pathogen invasion. For lower infective doses, there is a non-zero optimal killing rate for the pathogen that trades off the ability to kill its host with the possibility to cause additional critical exposures.

In earlier disease dynamics models, invasion conditions are sometimes given in terms of a critical colony size above which the pathogen can invade the host colony (Anderson and May, 1979). Large colonies with a dense interaction network should therefore be particu-

larly susceptible to pathogen invasions. These aspects enter our basic reproduction number in two ways: Via the colony size K and the contact rate r_c, contained in the combined parameter ζ. Clearly, the total contact rate with infectious cadavers, cK, will increase with colony size. The linear dependence on colony size K comes from our assumption that the host colony is sufficiently well mixed (see Section 2). However, nest architecture, and social and demographic structure of the colony is known to ameliorate the effect of colony size on pathogen transmission risk (Hock and Fefferman, 2012; Mersch et al., 2013; Pie et al., 2004). In realistic scenarios, the basic reproduction number (4) will not depend linearly on colony size; rather, K should be interpreted as an effective colony size that leads to cK cadaver contacts per infectious cadaver in one time unit.

High contact rates between individuals are an integral aspect of social insects and lead to a facilitated spread of pathogens through the colony. Our results show an ambivalence in the effect of high contact rates on the risk of a disease outbreak, since they need not increase the risk of an outbreak of the disease, but, on the contrary, can be to the advantage of the host colony. If the killing rate of the pathogen is below its optimal level, an increase of contact rates r_c among individuals dilutes the pathogen load in the colony. Individuals are thus less likely to exceed the infective dose and the risk of disease outbreak is decreased. Therefore, for some parameter combinations, physical contact between individuals can have a dilution effect and thus prevent the outbreak of a disease even in the absence of social immunity. This is likely to be an issue in biocontrol since the applied pathogens are often generalists and hence require high infective doses to kill their hosts. In these situations, predictions from traditional departmental models, e.g., Naug and Camazine (2002); Pie et al. (2004), are reversed.

Overall, our findings confirm many empirical studies on social immunity by corroborating the effectiveness of social immune defence mechanisms in host colonies. The dynamics of fungal infections and natural epidemics in host field populations are difficult to study.

Moreover, the particular life history of obligate killing entomopathogenic fungi has rarely been treated analytically (Stroeymeyt et al., 2014). Although there are many experimental studies describing the different mechanisms of social immunity Cremer et al. (2007), they are only very rarely linked to determining whether the pathogen can actually spread in a colony Stroeymeyt et al. (2014). Experimental studies often use small colonies, but the effect of entomopathogenic fungi at the population level that is relevant for biocontrol is only poorly understood. Hence, theoretical approaches can greatly benefit our understanding of disease dynamics of these pathogens.

5 Conclusion

Obligate killing entomopathogens are potent biocontrol agents, yet their characteristics are not adequately considered in theoretical models. Traditional compartmental models of disease dynamics suggest that successful pathogens evolve to become less deadly. However, our model predicts that obligate killing entomopathogenic fungi must induce a considerable risk of death in order to be evolutionarily successful. Their life histories make the killing rates and the rate at which the pathogens spread through the host colony important predictors for the pathogen's success in invading a host colony. The latter is determined by the rate of contact between hosts and their individual and social immune defences.

Biocontrol of social insects may be particularly complex. Their close interactions facilitate the spread of diseases through the colony if the pathogen can overcome collective and individual immune defences. However, these same interactions can dilute pathogen levels in the colony and hence reduce individual pathogen load below critical values. Even more, low-level infections may interfere with the predictions. Recently, it was shown that low-level infections with *Metarhizium* acquired by social contact in social insect colonies can lead to a protective immune stimulation Konrad et al. (2012). This may well be true also for

solitary individuals. However, in contrast to social insects where high contact rates lead to an increased spread of infectious particles, reduced contact between individuals in solitary insects will lead to a lower likelihood of contraction of such protective mini-infections.

Given the abundant use of obligate killing entomopathogens in biocontrol, it is crucial to understand the multitude of in part contrasting effects that come along with their particular life histories. A key for developing this understanding will be a combination of empirical studies and further specific epidemiological modelling.

Acknowledgements

We thank Nick Barton for discussion and advice throughout the progress of this work and Line V. Ugelvig, Barbara Casillas Perez, Rodrigo Redondo, and Carsten Marr, as well as an anonymous reviewer and the editor for their constructive comments that greatly improved the manuscript. This work has been funded by the European Research Council (ERC Advanced Grant no. 250152 to N.H. Barton and ERC Starting Grant no. 243071 to S. Cremer).

References

Almeida, J.E.M., Alves, S.B., Pereira, R.M., 1997. Selection of *Beauveria spp.* isolates for control of the termite *Heterotermes tenuis* (Hagen, 1858). Journal of Applied Entomology 121, 539–543.

Anderson, R.M., May, R.M., 1979. Population biology of infectious diseases: Part 1. Nature 280, 361.

Barbarin, A.M., Jenkins, N.E., Rajotte, E.G., Thomas, M.B., 2012. A preliminary evalua-

tion of the potential of *Beauveria bassiana* for bed bug control. Journal of Invertebrate Pathology 111, 82–85.

Blanford, S., Chan, B.H.K., Jenkins, N., Sim, D., Turner, R.J., Read, A.F., Thomas, M.B., 2005. Fungal pathogen reduces potential for malaria transmission. Science 308, 1638–1641.

Boomsma, J.J., Jensen, A.B., Meyling, N.V., Eilenberg, J., 2013. The evolutionary interaction networks of insect pathogenic fungi. Annual Review of Entomology 59, 467–485.

Chapman, R.E., Bourke, A.F.G., 2001. The influence of sociality on the conservation biology of social insects. Ecology Letters 4, 650–662.

Cremer, S., Armitage, S.A.O., Schmid-Hempel, P., 2007. Social immunity. Current Biology 17, R693–R702.

Cremer, S., Ugelvig, L.V., Drijfhout, F.P., Schlick-Steiner, B.C., Steiner, F.M., Seifert, B., Hughes, D.P., Schulz, A., Petersen, K.S., Konrad, H., Stauffer, C., Kiran, K., Espadaler, X., d'Ettore, P., Aktac, N., Eilenberg, J., Jones, G.R., Nash, D.R., Pedersen, J.S., J., B.J., 2008. The evolution of invasiveness in garden ants. PLoS One 3, e3838.

Diekmann, O., Heesterbeek, J.A.P., Roberts, M.G., 2010. The construction of next-generation matrices for compartmental epidemic models. Journal of the Royal Society Interface 7, 873–885.

Evans, J.D., Spivak, M., 2010. Socialized medicine: individual and communal disease barriers in honey bees. Journal of Invertebrate Pathology 103, S62–S72.

Heesterbeek, J.A.P., 2002. A brief history of R_0 and a recipe for its calculation. Acta Biotheoretica 50, 189–204.

Hethcote, H.W., 2000. The mathematics of infectious diseases. SIAM review 42, 599–653.

Hock, K., Fefferman, N.H., 2012. Social organization patterns can lower disease risk without associated disease avoidance or immunity. Ecological Complexity 12, 34–42.

Hughes, W.O.H., Eilenberg, J., Boomsma, J.J., 2002. Trade-offs in group living: transmission and disease resistance in leaf-cutting ants. Proceedings of the Royal Society of London. Series B: Biological Sciences 269, 1811–1819.

Hughes, W.O.H., Petersen, K.S., Ugelvig, L.V., Pedersen, D., Thomsen, L., Poulsen, M., Boomsma, J.J., 2004. Density-dependence and within-host competition in a semelparous parasite of leaf-cutting ants. BMC Evolutionary Biology 4, 45.

Hurwitz, A., 1895. Ueber die Bedingungen, unter welchen eine Gleichung nur Wurzeln mit negativen reellen Theilen besitzt. Mathematische Annalen 46, 273–284.

Jaccoud, D.B., Hughes, W.O.H., Jackson, C.W., 1999. The epizootiology of a *Metarhizium* infection in mini-nests of the leaf-cutting ant *Atta sexdens rubropilosa*. Entomologia Experimentalis et Applicata 93, 51–61.

Konrad, M., Vyleta, M.L., Theis, F.J., Stock, M., Tragust, S., Klatt, M., Drescher, V., Marr, C., Ugelvig, L.V., Cremer, S., 2012. Social transfer of pathogenic fungus promotes active immunisation in ant colonies. PLoS Biology 10, e1001300.

Lowe, S., Browne, M., Boudjelas, S., De Poorter, M., 2000. 100 of the world's worst invasive alien species: a selection from the global invasive species database. Invasive Species Specialist Group Species Survival Commission, World Conservation Union (IUCN), Auckland, New Zealand.

May, R.M., Gupta, S., McLean, A.R., 2001. Infectious disease dynamics: what characterizes a successful invader? Philosophical Transactions of the Royal Society of London. Series B: Biological Sciences 356, 901–910.

Mersch, D., Crespi, A., Keller, L., 2013. Tracking individuals shows spatial fidelity is a key regulator of ant social organization. Science 340, 1090–1093.

Milutinović, B., Stolpe, C., Peuβ, R., Armitage, S.A.O., Kurtz, J., 2013. The red flour beetle as a model for bacterial oral infections. PLoS One 8, e64638.

Naug, D., Camazine, S., 2002. The role of colony organization on pathogen transmission in social insects. Journal of Theoretical Biology 215, 427–439.

Pie, M.R., Rosengaus, R.B., Traniello, J.F.A., 2004. Nest architecture, activity pattern, worker density and the dynamics of disease transmission in social insects. Journal of Theoretical Biology 226, 45–51.

Pimentel, D., Lach, L., Zuniga, R., Morrison, D., 2000. Environmental and economic costs of nonindigenous species in the United States. BioScience 50, 53–65.

Rosengaus, R.B., Traniello, J.F.A., Chen, T., Brown, J.J., Karp, R.D., 1999. Immunity in a social insect. Naturwissenschaften 86, 588–591.

Routh, E.J., 1877. A treatise on the stability of motion. Macmillima, London .

Schmid-Hempel, P., 1998. Parasites in social insects. Princeton University Press.

Schmid-Hempel, P., Frank, S.A., 2007. Pathogenesis, virulence, and infective dose. PLoS Pathogens 3, e147.

Scholte, E.J., Ng'habi, K., Kihonda, J., Takken, W., Paaijmans, K., Abdulla, S., Killeen, G.F., Knols, B.G.J., 2005. An entomopathogenic fungus for control of adult african malaria mosquitoes. Science 308, 1641–1642.

Stroeymeyt, N., Casillas Perez, B., Cremer, S., 2014. Organisational immunity in social insects. Current Opinion in Insect Science in revision.

Thomas, M.B., Read, A.F., 2007. Can fungal biopesticides control malaria? Nature Reviews Microbiology 5, 377–383.

Tragust, S., Mitteregger, B., Barone, V., Konrad, M., Ugelvig, L.V., Cremer, S., 2012. Ants disinfect fungus-exposed brood by oral uptake and spread of their poison. Current Biology .

Vestergaard, S., Butt, T.M., Bresciani, J., Gillespie, A.T., Eilenberg, J., 1999. Light and electron microscopy studies of the infection of the western flower thrips *Frankliniella occidentalis (Thysanoptera: Thripidae)* by the entomopathogenic fungus *Metarhizium anisopliae*. Journal of Invertebrate Pathology 73, 25–33.

Vestergaard, S., Gillespie, A.T., Butt, T.M., Schreiter, G., Eilenberg, J., 1995. Pathogenicity of the hyphomycete fungi *Verticillium lecanii* and *Metarhizium anisopliae* to the western flower thrips, *Frankliniella occidentalis*. Biocontrol Science and Technology 5, 185–192.

Wilson, K., Thomas, M.B., Blanford, S., Doggett, M., Simpson, S.J., Moore, S.L., 2002. Coping with crowds: density-dependent disease resistance in desert locusts. Proceedings of the National Academy of Sciences 99, 5471.

Wilson-Rich, N., Spivak, M., Fefferman, N.H., Starks, P.T., 2009. Genetic, individual, and group facilitation of disease resistance in insect societies. Annual Review of Entomology 54, 405–423.

Zimmermann, G., 2007. Review on safety of the entomopathogenic fungus *Metarhizium anisopliae*. Biocontrol Science and Technology 17, 879–920.

A Simulation settings

A.1 Matrix specifications

In simulations, each entry of the vectors $\mathbf{G}^x$ and matrices $\mathbf{S}^x$ needs to be specified. To reduce this enormous number of parameters to three only (p_s, p_a and r_a, see below), we specify the $\mathbf{G}^x$ and $\mathbf{S}^x$ as follows.

The individual immunity vectors $\mathbf{G}^x$ By means of individual immunity, hosts have a chance to reduce their own pathogen load. For x_{max} large enough, it makes sense to assume a binomial model. If X_s denotes the number of pathogens removed by means of individual immunity and p_s the chance of removing a particular conidiospore, then

$$\mathbb{P}_z[X_s = k] = \binom{z}{k} p_s^k \, (1 - p_s)^{z-k}$$

is the probability for an individual carrying z conidiospores to remove k conidiospores. Thus

$$G_z^x := \mathbb{P}_z[X_s = z - x] \tag{A.1}$$

is the transition probability from reducing a pathogen load of z to x ($z \geq x$) by individual immunity.

The social matrices $\mathbf{S}^x$ Contact between individuals leads to a spread of the pathogen. Ignoring the possibility of sanitary actions, let κ_{zy}^x denote the probability that a host, that has contact with an individual with pathogen load y, is moved from the class of pathogen load z to the class of pathogen load x. On both individuals, a certain number of infectious particles, k_z and k_y, detach. A certain amount of those, determined by the random variable V, reattach to the focal individual, whereas the remaining particles attach to the second

individual. Therefore, set

$$\kappa_{zy}^{x} = \sum_{k_z=0}^{z} \sum_{k_y=0}^{y} \mathbb{P}[U_z = k_z]\mathbb{P}[U_y = k_y]\mathbb{P}\left[V = x - z + k_z\right], \tag{A.2}$$

where $U_i \sim B(i, p_c)$, i.e., the random variables U_i are binomially distributed with i trials and success probability p_c, the probability that one particular unit of infectious particles detaches, and V follows a hypergeometric distribution

$$\mathbb{P}[V = s] = \frac{\binom{x_{max}-z+k_z}{s}\binom{x_{max}-y+k_y}{k_z+k_y-s}}{\binom{2x_{max}-(z+y)+k_z+k_y}{k_z+k_y}}.$$

This choice of distributions ensures that the total pathogen load has the tendency to spread out, but it remains constant and no individual ends up with a pathogenic load higher than x_{max}.

Social contact can be accompanied by sanitary actions. Let τ_{zy}^{x} denote the probability that a host, that has contact with and is treated by an individual with exposure load y, is moved from the class of pathogen load z to the class of pathogen load x. Set

$$\tau_{zy}^{x} = \sum_{j} \mathbb{P}[Y_z = j]\kappa_{zy}^{x+j}, \tag{A.3}$$

where $Y_z \sim B(z, p_a)$, i.e., the random variables Y_z are binomially distributed with z trials and success probability p_a, the probability that one particular unit of pathogen is removed by social immunity measures.

Finally, define r_a as the fraction of contact events between two hosts that involve sanitary actions. Then, the social interaction matrices are obtained from weighting (A.2) and (A.3) accordingly. They take the form

$$\mathbf{S}_{jk}^{x} = \left(1 - r_a(j)\right)\kappa_{jk}^{x} + r_a(j)g_{jk}^{x}. \tag{A.4}$$

A.2 Simulation parameters

For all simulations, we specified $\lambda(\mathbf{n}) = \lambda_0 N(K - N)$ by a logistic growth function with free growth rate λ_0. For Figures 2 to 4, G_z^x and S_{zy}^x are given by equations (A.1) and (A.4), respectively.

Figure 1 The simulations were initialized by setting $n_0(0) = 1$, $n_1(0) = n_2(0) = 0$, $\nu(0) = 10^{-5}$. Values for c, η, and σ_2 were chosen randomly between zero and one to obtain 10^5 independent data points. The remaining parameters are:

$$\lambda = 0, \quad \sigma_0 = \sigma_1 = 0, \quad r_c = r_s = 1,$$

$$\mathbf{G}^0 = \begin{pmatrix} 1 \\ 0.01 \\ 0.0001 \end{pmatrix}, \quad \mathbf{G}^1 = \begin{pmatrix} 0 \\ 0.99 \\ 0.01 \end{pmatrix}, \quad \mathbf{G}^2 = \begin{pmatrix} 0 \\ 0 \\ 0.9899 \end{pmatrix},$$

$$\mathbf{S}^0 = \begin{pmatrix} 1 & 0.99 & 0.99 \\ 0.1 & 0.099 & 0.108 \\ 0.1 & 0.108 & 0.117 \end{pmatrix}, \quad \mathbf{S}^1 = \begin{pmatrix} 0 & 0.01 & 0.0099 \\ 0.9 & 0.892 & 0.88308 \\ 0.09 & 0.0892 & 0.088308 \end{pmatrix},$$

$$\mathbf{S}^2 = \begin{pmatrix} 0 & 0 & 0.0001 \\ 0 & 0.009 & 0.00892 \\ 0.81 & 0.8028 & 0.794692 \end{pmatrix}.$$

Figure 2 The stability of the Jacobian matrix at the pathogen-free equilibrium $\mathbf{E}$, given by $n_0(0) = K$, $n_x(0) = 0$ for $0 < x \leq x_{max}$, and $\nu = 0$, is evaluated numerically for η and cK ranging from 0 to 5 at a resolution of 100 points. The killing rate is (a) $\bar{\sigma} = 0.5$ and (b) $\bar{\sigma} = 5$. The remaining parameters are $x_{max} = 10$, $x_{crit} = 5$, $K = 1$, $\lambda_0 = 1$, $r_c = r_s = 1$,

$r_a = 0.75$, $p_c = p_s = 0.1$, and $p_a = 0.2$.

Figure 3 The stability of the Jacobian matrix at the pathogen-free equilibrium **E**, given by $n_0(0) = K$, $n_x(0) = 0$ for $0 < x \leq x_{max}$, and $\nu = 0$, is evaluated numerically for $\bar{\sigma}$ and $\alpha = cK/\eta$ ranging from 0 to 5 at a resolution of 100 points. In (a), $r_c = r_a = 1$, while in (b), $r_c = r_a = 4$. The remaining parameters for (a) and (b) are $x_{max} = 10$, $x_{crit} = 5$, $K = 1$, $\lambda_0 = 1$, $\eta = 1$, $r_a = 0.75$, $p_c = p_s = 0.1$, and $p_a = 0.2$.

For (c) and (d), we set all parameters connected to active disease defence (i.e., r_s, r_a, p_s, and p_a) to zero. Furthermore, we set (c) $r_c = 2$ and (d) $r_c = 4$. The remaining parameters remain unchanged.

Figure 4 The stability of the Jacobian matrix at the pathogen-free equilibrium **E**, given by $n_0(0) = K$, $n_x(0) = 0$ for $0 < x \leq x_{max}$, and $\nu = 0$, is evaluated numerically for $\bar{\sigma}$ and $\alpha = cK/\eta$ ranging from 0 to 5 at a resolution of 200 points. The rates of contact are (a) $r_c = 1$ and (b) $r_c = 3$. The remaining parameters are $x_{max} = 10$, $x_{crit} = 2$, $K = 1$, $\lambda_0 = 1$, $\eta = 1$, $r_s = 1$, $r_a = 0$, $p_c = 0.9$, $p_s = 0.1$, and $p_a = 0$.